ELSEVIER

NeuroImage

www.elsevier.com/locate/ynimg
NeuroImage 29 (2006) 1224 – 1230

A curvature-based approach to estimate local gyrification on the cortical surface

E. Luders,[a] P.M. Thompson,[a] K.L. Narr,[a] A.W. Toga,[a,*] L. Jancke,[b] and C. Gaser[c]

[a]*Laboratory of Neuro Imaging, Department of Neurology, UCLA School of Medicine, 710 Westwood Plaza, 4238 Reed, Los Angeles, CA 90095-1769, USA*
[b]*Department of Neuropsychology, University of Zurich, Switzerland*
[c]*Department of Psychiatry, University of Jena, Germany*

Received 5 February 2005; revised 23 August 2005; accepted 31 August 2005
Available online 11 October 2005

Using magnetic resonance imaging and a new method to analyze local surface shape, we examined the effects of gender on gyrification in a large and well-matched sample of healthy subjects. Unlike traditional 2D methods that produce whole-brain measurements of cortical complexity or more sophisticated 3D parametric mesh-based techniques that allow only different sections (lobes) of the cortex to be investigated, we employed a novel approach with increased spatial resolution. Although our method is sensitive to similar cortical features like the classic whole-brain gyrification index (depths of sulci and heights of gyri), we are now able to provide detailed and regionally specific estimates of cortical convolution at thousands of points across the cortical surface without introducing any bias through the rater or the selected orientation of the slices. We revealed pronounced gender differences, showing increased gyrification in frontal and parietal regions in females compared to males that agree with recent regions-of-interest findings. In addition, we detected higher female gyrification in temporal and occipital cortices that was not previously identified in studies using more global measures. No cortical area was significantly more convoluted in males compared to females. Our results demonstrate the sensitivity of this automated approach for identifying very local changes in gyrification. This technique may serve to isolate regionally specific changes in fissuration/gyrification in neurodevelopmental or neuropsychiatric disorders.

Keywords: Cortex; Sex; Gender; Mapping; MRI; Curvature

Introduction

Brain expansion is partly constrained by the size of the intracranial cavity during neurodevelopment (Hofman, 1989; Van Essen, 1997; Courchesne et al., 2000), so gender-specific patterns of cortical folding are likely influenced by smaller female skull sizes. Traditional postmortem and in vivo morphometric studies have used several unique approaches to examine cortical complexity and to establish the presence and direction of gender differences in sulcal/gyral convolutions. Measuring cortical folding in postmortem data with a 2D gyrification index (i.e. the ratio between deep and superficial cortex in coronal sections) revealed no differences between men and women (Zilles et al., 1988). Similarly, no gender differences were identified in an in vivo study defining whole-brain surface complexity as the ratio of total cortical surface area to overall brain volume, raised to the 2/3 power (Nopoulos et al., 2000). However, another MRI investigation used surface-to-volume ratios to calculate a fissurization index for the hemispheres and cingulate cortices. This study detected a hemisphere by gender interaction, reflecting increased asymmetries of fissurization in male brains (Yucel et al., 2001). Moreover, using a sophisticated 3D parametric mesh-based approach (Thompson et al., 1996a,b) applied to five functionally relevant cortical regions, our group demonstrated that females exhibit greater cortical complexity than males in frontal and parietal regions (Luders et al., 2004).

Overall, empirical data concerning sex-related differences in cortical complexity or gyrification are sparse, and findings lack consistency, where discrepancies may stem from differences in measurement methods (e.g. postmortem vs. in vivo, 2D vs. 3D). Available data, however, suggest that the ability to detect gender-specific differences in gyrification increases by shifting focus from global (e.g. whole brain) to more regional examinations (e.g. frontal lobe). Region-of-interest (ROI) analysis appears to be the most spatially detailed method used to date. However, using ROIs defined a priori limits the identification of changes elsewhere in the cortex, may introduce user bias and makes it impractical to study large populations given that manual delineations are labor-intensive.

In order to circumvent these potential limitations, we applied a refined and automated whole-brain approach for estimating regional differences in cortical surface convolution. Specifically, we computed the degree of convolution across the entire cortex at

* Corresponding author. Fax: +1 310 206 5518.
E-mail address: toga@loni.ucla.edu (A.W. Toga).
Available online on ScienceDirect (www.sciencedirect.com).

1053-8119/$ - see front matter © 2005 Elsevier Inc. All rights reserved.
doi:10.1016/j.neuroimage.2005.08.049

thousands of surface points in order to provide color-coded maps indexing the local gyrification. We hypothesized that gender-specific differences in gyrification would exist in numerous cortical regions that would complement and extend existing knowledge from studies using less spatially detailed methods. In order to confirm correspondences with results achieved through a lower resolution parametric mesh-based approach (Thompson et al., 1996a,b), we examined local gyrification in the same sample as analyzed in a previously published study (Luders et al., 2004).

Materials and methods

Subjects

We analyzed the brain scans of 60 young and right-handed subjects that were selected from a database of high-resolution anatomical MR images acquired at the Center for Neuroscientific Innovation and Technology (ZENIT), Magdeburg. Subjects were matched for biological sex (30 women, 30 men) and age (women: 24.32 ± 4.35 years; men: 25.45 ± 4.72 years). Handedness was determined by referring to self-reports of hand preference. Subjects were healthy volunteers and included university students from different fields who were recruited via notice board and/or Internet advertisements. All subjects gave informed consent according to institutional guidelines (Ethics Committee of the University of Magdeburg).

MRI acquisition

Images were obtained on a 1.5-T MRI system (General Electric, Waukesha, WI, USA) using a T1-weighted spoiled gradient echo pulse sequence with the following parameters: TR = 24 ms, TE = 8 ms, 30° flip angle, FOV = 250 × 250 mm^2, matrix size = 256 × 256 × 124, voxel size = 0.98 × 0.98 × 1.5 mm.

Cortex extraction

Image volumes passed through a number of preprocessing steps using mostly automated procedures. First, we created an intracranial mask of the brain using a brain surface extraction algorithm tool (BSE) that is based on a combination of non-linear smoothing, edge finding and morphologic processing (Shattuck and Leahy, 2002). Any small errors in the masks were corrected manually to isolate intracranial regions from surrounding extracranial tissue and extra-cortical cerebrospinal fluid (CSF). Brain masks and anatomical images were corrected for head position and individual differences in brain size by using an automatic 12-parameter linear registration (Woods et al., 1998) to transform each brain volume into the target space of the ICBM-305 average brain created by the International Consortium for Brain Mapping (Mazziotta et al., 1995). To eliminate intensity drifts due to magnetic field inhomogeneities in the anatomical brain images, we employed radio-frequency bias field corrections (Sled et al., 1998). Finally, we applied the normalized brain masks (that include cerebral tissue only) to the normalized anatomical brain images and created a spherically parameterized mesh model of the cortical surface using signal intensity information. Each of these individual meshes in ICBM-305 space was continuously deformed to fit the threshold intensity value which best differentiated extra-cortical cerebrospinal fluid from underlying cortical gray matter (MacDonald et al., 1994).

Measures of local gyrification

The local gyrification is revealed through estimations of "smoothed absolute mean curvature," based on averaging curvature values from each vertex of the spherical surface mesh within a distance of 3 mm followed by calculating the absolute value of the resulting number within this region and smoothing over 25 mm. A detailed explanation is given in the following paragraphs and Fig. 1.

The meshes model the cortical surface of the brain consisting of gyri and sulci. We used these meshes to calculate the mean curvature (do Carmo, 1976) at thousands of points across the cortical surface. Mean curvature is an extrinsic surface measure and gives information about the change in normal direction along the surface (normals are vectors pointing outwards perpendicular to the surface). Mean curvature at a given point is defined as

$$T_{\text{curvature}} = \sum_{v=1}^{n_v} \left(\frac{(\tilde{x}_v - \tilde{x}_v) \cdot \tilde{N}_v}{B_v} \right)^2$$

where $\tilde{x}_v$ is the centroid of its neighbors of vertex v, B_v is the average distance from the centroid of each of the neighbors, and $\cdot$ is the vector product operator (MacDonald: A Method for Identifying Geometrically Simple Surfaces from Three Dimensional Images. PhD Thesis McGill University, Montreal). The resulting values of the mean curvature measurement can be expressed either in radians or degrees ranging from −180 to 180 (we will use degrees throughout this paper). Large negative values correspond to sulci and large positive values to gyri. To increase the signal to noise ratio for the curvature measure at a given vertex, we averaged the curvature values within a distance of 3 mm on the cortical surface and calculated the absolute value of the resulting number within this region. The absolute values of mean curvature (hereafter referred to as absolute mean curvature) are always above zero for both gyri and sulci and express the local amount of gyrification. Finally, absolute mean curvature values were smoothed using a surface-based heat kernel smoothing filter (Chung et al., 2005) of full width at half maximum (FWHM) of 25 mm, where the width of the smoothing filter was chosen according to the matched filter theorem. That is, the spatial frequency of the sulcus–gyrus pattern suggests a filter that optimally enhances features in the range of the distance between sulci and gyri, which is about 20–30 mm.

Furthermore, we calculated the total surface area and the total absolute mean curvature of the mesh models in ICBM-305 space (after spatial normalization). In order to approximate the impact of spatial normalization on our curvature-based measurements, we calculated absolute mean curvature and smoothed absolute mean curvature of one brain in its native dimension (unscaled image) and after spatial normalization (scaled image). For this purpose, we simulated the scaling of the brain by using a scaling factor of 1.25 along the x, y, and z dimensions, which resulted in a change of volume of almost 200% and a change in surface area of about 150%.

Statistical analyses

We linearly averaged the curvature values from each surface mesh point in the male and female group followed by computing the mean difference between males and females (Fig. 2). Statistical differences of local curvature values between male and female group were obtained using a general linear model applied to each

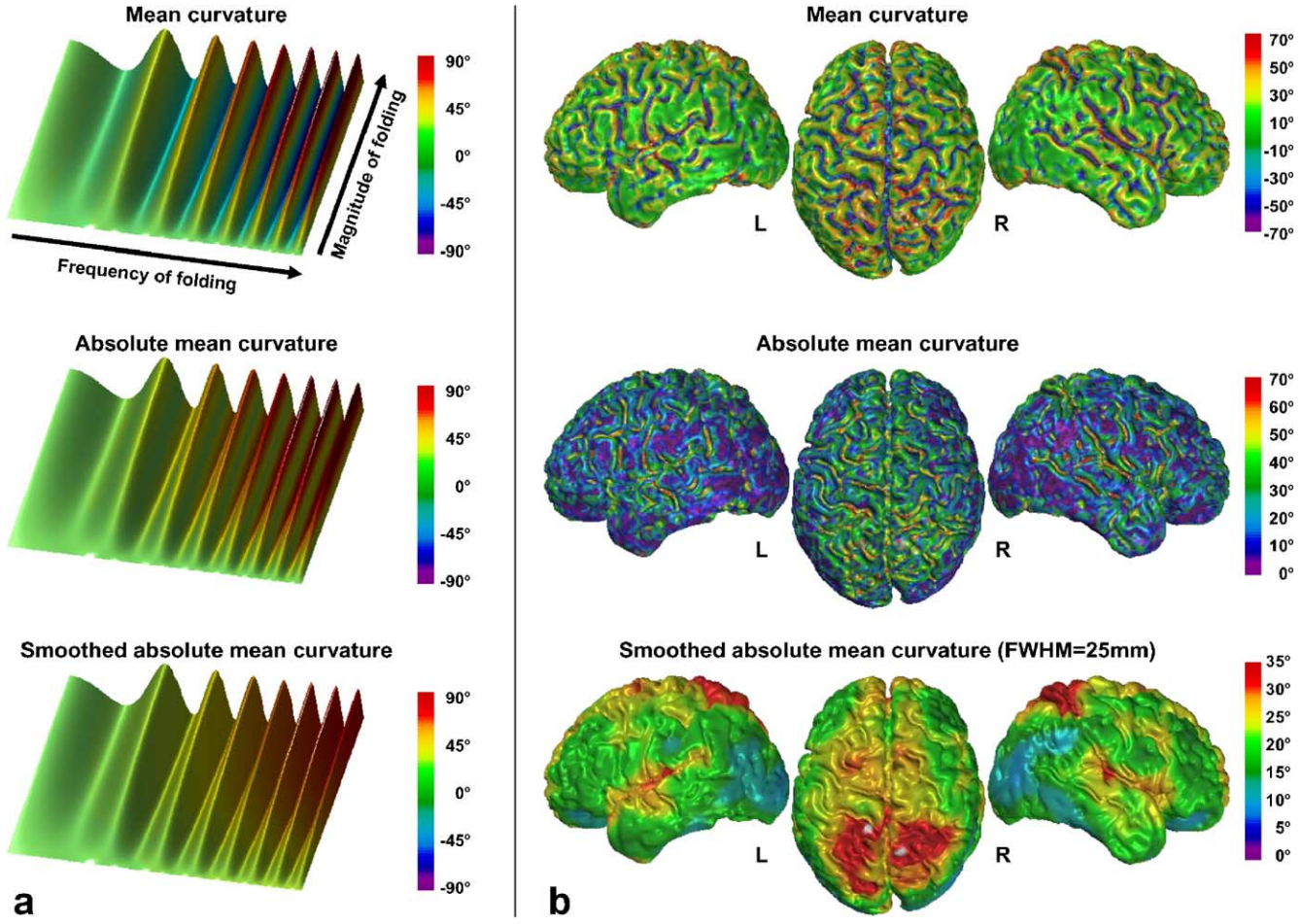

Fig. 1. Estimation of local gyrification. The left column demonstrates the computation of local gyrification using a simulated folded surface, where the magnitude of the folding increases from proximal to distal and the wavelength from left to right. The calculation of the mean curvature results in large positive values for local maxima (corresponding to gyri) and large negative values for local minima (corresponding to sulci), where curvature values are expressed in degrees. By calculating the absolute mean curvature, all values are converted into positive values. Finally, curvature values are smoothed using a surface-based heat kernel filter with FWHM = 25 mm. As demonstrated, increases in the amplitude and frequency of the simulated folding are reflected in increased values of smoothed absolute mean curvature. The right column illustrates the process of estimating local gyrification on a single subject brain selected from the sample analyzed in this study. In the first step, the mean curvature is calculated using the 3D mesh of the cortical surface. Sulci can be identified through large negative values (displayed in dark green, blue and purple), while gyri are characterized by large positive values (displayed in light green, yellow and red). After calculating the absolute mean curvature, all values are transformed into positive values regardless of whether they represent gyri or sulci. Final surface smoothing with a heat kernel (FWHM = 25 mm) reveals higher values for areas with pronounced gyrification.

corresponding mesh point of the cortical surface. The resulting t values were thresholded at a P value of $P < 0.05$ and corrected for multiple comparisons using False Discovery Rate (Benjamini and Hochberg, 1995). In addition, we compared the total surface area of the cortex in ICBM-305 space between females and males using a one-tailed two-sample t test. Finally, we computed the Spearman correlation coefficient between total surface area and total absolute mean curvature.

Results

Fig. 2 shows the average distributions of local gyrification in ICBM-305 stereotaxic space for females (first row) and males (second row). The highest local gyrification in both men and women appears to be located in the left and right parietal lobes between midline and intraparietal sulcus, as well as in the left superior frontal cortex and bilaterally along the precentral sulcus in women, and to a lesser degree also in men. Another small region exhibiting extremely high gyrification was detected at the inferior part of the central sulcus (in both hemispheres and sexes). The lowest gyrification in the left and right hemispheres appears surrounding the occipital poles and expanding into the inferior temporal gyrus, with lower mean gyrification values in males than in females.

As further illustrated in Fig. 2 (third and fourth row), the largest differences between males and females are found in anterior regions of the frontal lobe, with more pronounced gender effects in the left hemisphere than in the right. Large clusters showing significantly increased gyrification in females were also detected in anterior and posterior parts of the left and right temporal lobes, as well as in the occipital lobes (appearing slightly more pronounced in the right hemisphere than in the left). In addition, two regions in the parietal lobes (covering inferior parts of the right postcentral sulcus and superior parts of the left and right postcentral gyrus) appeared more convoluted in females compared to males. We did

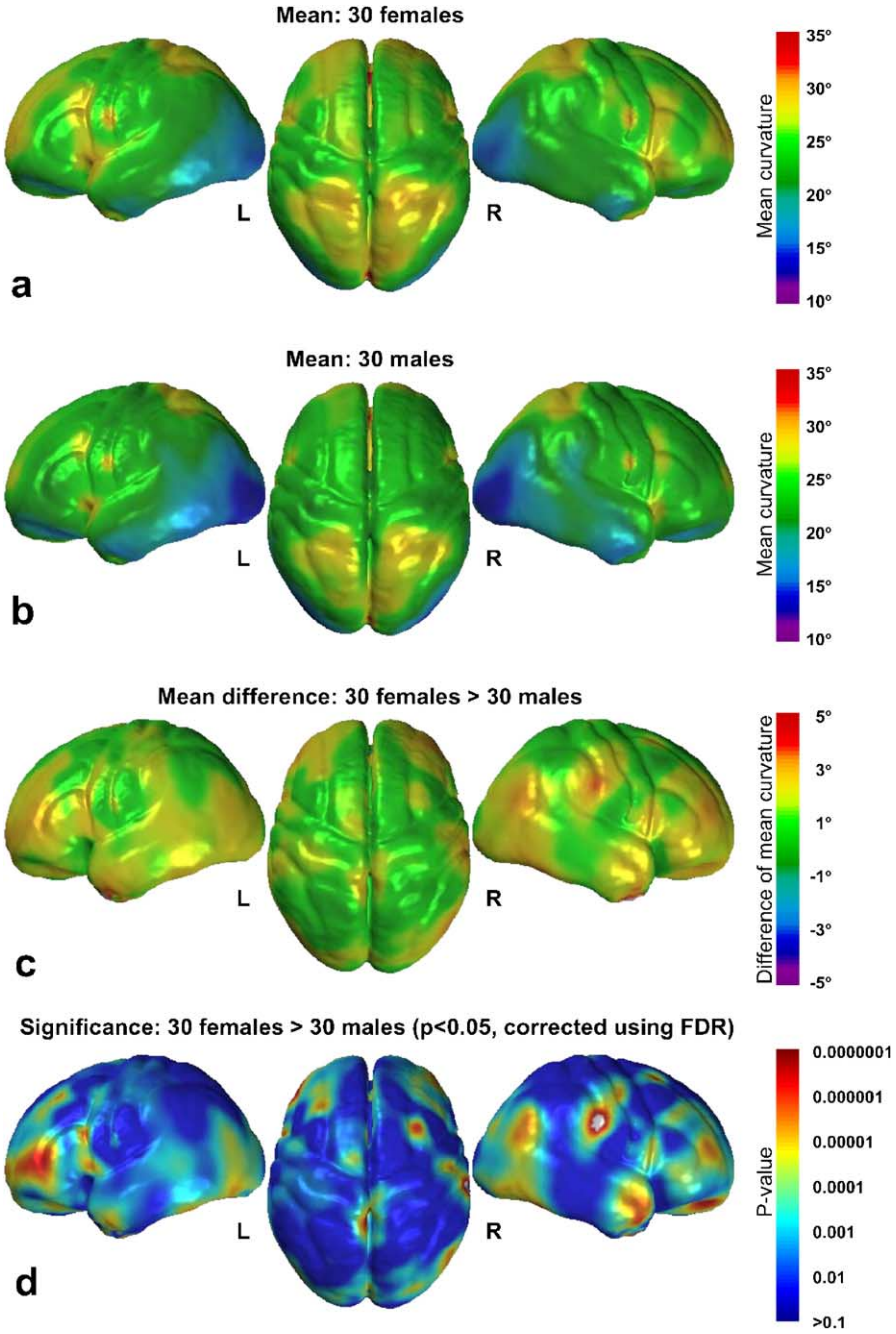

Fig. 2. Results of local gyrification measurements. The two upper rows (a, b) demonstrate the average distribution of local gyrification in males and females, where curvature values are expressed in degrees. The third row (c) reveals the mean differences between males and females. Areas with higher gyrification in females than males appear in yellow and red, whereas blue and purple would indicate lower gyrification in females. The fourth row (d) illustrates regions of significantly increased gyrification in females compared to males ($P < 0.05$), corrected for multiple comparisons using False Discovery Rate (FDR).

not detect any cortical region showing significantly increased gyrification in men compared to women.

The total surface area of the cortex was significantly larger in females compared to males ($P < 0.007$, females: 1051.41 ± 42.75 cm^2, males: 1026.07 ± 34.24 cm^2) after transforming images into standard ICBM-305 space by applying 12-parameter transformations. The Spearman correlation coefficient between total surface area and absolute mean curvature for the whole sample was 0.917 ($P < 0.001$) (Fig. 3). The simulated scaling of one brain resulted in a change of absolute mean curvature by a factor of 0.812, while smoothed absolute mean curvature changed by a factor of 0.895. That is, a volume increase of almost 200% would be accompanied by an 11% decrease in curvature.

Discussion

In this study, we present a new method for estimating a local gyrification index. Our approach is related to formerly described calculations of curvature indices (CI) (Magnotta et al., 1999;

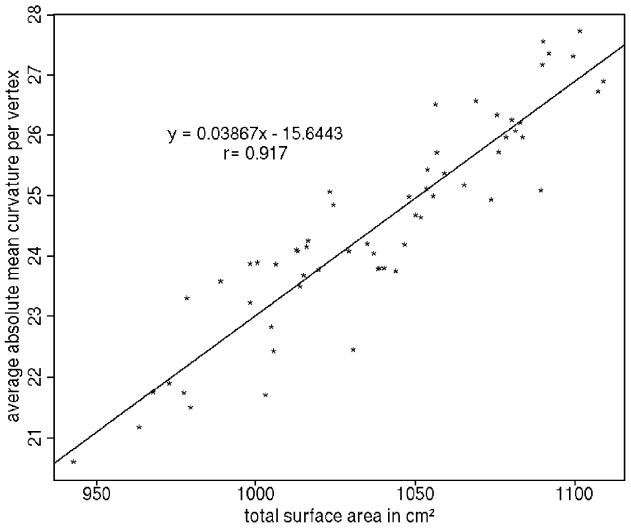

Fig. 3. Correlation between total surface area and total absolute mean curvature. This plot shows the strong relationship between total surface area of the cortical mesh model and the average of the absolute mean curvatures from each vertex of the mesh.

Nopoulos et al., 2000). However, in contrast to measuring whole-brain sulcal and gyral CIs as implemented previously, we computed the degree of convolution across the entire cortex at thousands of surface points. Our approach further complements traditional methods that produce global measures of gyrification (Zilles et al., 1988; Yucel et al., 2001) and our previously reported approach providing only regional measures of cortical complexity for lobar regions of the cortex (Thompson et al., 1996a,b; Luders et al., 2004).

Relation to other approaches

Usually, the classic whole-brain gyrification index is estimated by calculating the ratio between the lengths of the inner and outer contour of the cortex in coronal slices (Zilles et al., 1988; Yucel et al., 2001). The inner contour exactly follows the peaks and troughs of the sulci and gyri, while the outer contour connects the tops of the gyri using the convex contour with least enclosed area (without following the sulci). The relation of our approach to the classical version of the whole-brain gyrification index can be described as follows: analogous to the inner and outer contours establishing the classic gyrification index, our cortical mesh models comprise inner and outer surfaces. More specifically, the inner surface is approximated by the total surface area of our cortical meshes, while the outer surface is assumed to be relatively constant over all subjects after spatial normalization. Consequently, the total surface area (the inner surface of the cortex) is suggested to be proportional to the 3D extension of the gyrification index (the ratio between the inner and outer contour of the cortex). Such a relationship between total surface area and gyrification index not only exists on a global level of the whole cortex but also on a local level at each point of the cortical surface. Given that the present analysis revealed a strong correlation between total surface area and total absolute mean curvature (Fig. 3), absolute mean curvature appears to be a suitable means to estimate gyrification on a global and local level.

The classical approach requires manual tracing that is highly time-consuming, and the gyrification measurement is affected by the orientation of brain slices selected for tracing the contours. In contrast, our newly proposed method works almost fully automatically without introducing any bias from the rater or slice orientation. Because of the excellent spatial resolution, our new method furnishes extremely local measures of convolution that clearly distinguish males from female subjects in a young and healthy group. Moreover, as demonstrated in Fig. 1, there is a good correspondence between mean curvature and cortical folding; increases in the amplitude and frequency of the folding are reflected in increased values of smoothed absolute mean curvature (Fig. 1). Our approach may also serve to identify regional changes in gyrification that occur during neurodevelopment (Blanton et al., 2001) or that manifest as the result of disease (Narr et al., 2004). In addition, gyrification measures may be associated with other measures made point-wise throughout the cortex, such as gray matter (GM) distribution or cortical thickness (Good et al., 2001; Sowell et al., 2004; Narr et al., 2005), that may further elucidate sex differences in brain morphology or neuropathological processes in individuals with neurodegenerative or neuropsychiatric disorders. In fact, a recent study revealed a positive correlation between cortical thickness and whole-brain cortical complexity in normal subjects (Thompson et al., 2005).

Potential confounds

The problem of ‘buried cortex’ is discussed extensively in Magnotta et al. (1999), emphasizing the difficulty to accurately extract the cortical surface when deep infolding occurs or when sulcal invaginations are filled with cerebrospinal fluid. Clearly, sophisticated surface extraction tools that better reach the bottom of sulci will improve the accuracy of “mean curvature” as a valid indicator for the convolution of the surface. Given that there are multiple approaches that are viable and commonly used, future studies remain to be conducted to establish whether group-specific outcomes are altered significantly in dependence of the applied surface modeling. For example, using the WM surface versus the GM surface might lead to different results. Notwithstanding, since one of the primary goals of the present manuscript was to validate the newly developed voxel-wise approach, we decided to use exactly the same cortical surface models as in a former ROI analysis (Luders et al., 2004), which was based on the algorithm developed by MacDonald et al. (1994).

Another potential confound could result from the analysis of gyrification in scaled spherical meshes of the cortical surface in ICBM-305 space. Here, we provide evidence that spatial transformations into ICBM-305 space, using 12 parameters, alter the volume and surface area of the brains, but not significantly the degree of gyrification. Notably, volume increases as large as almost 200% would be accompanied by curvature decreases of only 11%. Thus, our findings indicate that mean curvature is relatively invariant to affine transforms, and differences between groups would be similar in native space and dimensions.

Correspondence with previous findings

In this study, by comparing local differences in gyrification between men and women, we found pronounced gender differences. Although these findings conflict with some previous examinations that failed to detect significant gender differences in gyrification or fissurization indices (Zilles et al., 1988; Nopoulos et al., 2000; Yucel et al., 2001), our findings corroborate other recently published results demonstrating increased complexity in

females (Luders et al., 2004). The earlier studies that detected no gender differences only assessed cortical convolution or complexity by investigating the whole brain or the hemispheres individually. But, pronounced gender effects in the magnitude of complexity and gyrification appear detectable in later studies where more regional analyses are performed at a lobar or voxel level spanning the whole cortical surface. In our prior lobar analysis (Luders et al., 2004), we detected an increased complexity in females in the frontal and parietal lobes. These gender differences were also evident in the current study. However, our statistical maps demonstrating sex-related differences in gyrification (Fig. 2) showed improved regional specificity for gyrification differences surrounding the frontal pole and inferior/superior frontal sulci. Similarly, larger clusters of significantly increased gyrification were observed in the parietal lobe that appear restricted to inferior parts of the right postcentral sulcus and superior parts of the left and right postcentral gyrus. Interestingly, the present study also revealed a higher female gyrification in cortical regions that did not reach significance in our previous study examining complexity collapsed over lobar regions (temporal and occipital lobes). However, in the current analysis, increased gyrification was predominantly observed in anterior and posterior parts of the left and right temporal lobes that constitute only a portion of the whole temporal lobe. Thus, since gyrification appears similar between males and females for a substantial portion of the temporal cortex, it is likely that global changes in gyrification were not detected previously. Results therefore suggest that the current approach is a more powerful means to characterize highly localized differences in gyrification. Our findings complement and refine previously reported gender effects using whole-brain, hemisphere or lobar level analyses where localized gender effects may have remained undetected. Conversely, it is surprising that the present analysis showed increased gyrification in large parts of the occipital lobe in female compared to male brains, while previously no sex differences were observed in this lobar region overall (Luders et al., 2004). Methodological differences may account for these discrepancies. While our earlier approach, described in detail elsewhere (Thompson et al., 1996a,b), reflects the fractal nature of gyral folding and sulcal fissuration, the current approach appears to be more sensitive to the magnitude of convolution (depths of sulci and heights of gyri) (Fig. 1). Nevertheless, both approaches confirm that numerous regions in female brains show an increased gyrification, while males show no regional increases compared to females.

Functional implications and morphogenesis

Sulcal/gyral formation is influenced by the underlying cytoarchitecture of the cortex (Rademacher et al., 1993; Watson et al., 1993; Roland and Zilles, 1994). Furthermore, gyrification is thought to be influenced by neural connectivity (Caviness, 1975; Goldman-Rakic, 1981; Rakic, 1988) and to change as a function of the volumetric ratio between outer and inner cortical layers (Richman et al., 1975); greater folding complexities accompany higher intracortical connectivities (originating in outer cortical layers) and smaller descending projections (originating in inner cortical layers) (Rilling and Insel, 1999). Sexually dimorphic information processing strategies might develop as a result of differences in the underlying cytoarchitecture and neural connectivity of specific brain regions. Thus, it is possible that different gyrification patterns have functional significance and may account for gender-specific abilities and/or behavioral differences between men and women (Halpern, 1992; Kimura, 1999).

Regardless of the functional implications or significance of increased gyrification, there remains the challenging question of its morphogenesis. Several theories implicate factors intrinsic to the cortex in the primary mechanism of folding. For example, it was proposed that greater expansion of outer vs. inner cortical layers causes gyrification (Richman et al., 1975). Another theory suggests that cortical folding results from the development of intracortical connections (Rakic, 1988). Finally, tension along axons was proposed to produce gyri between strongly connected cortical regions and sulci between weakly connected regions (Van Essen, 1997). Gyral formation begins around 16 weeks in utero, and most cortical folding is principally defined in the late second and third trimesters of fetal life (Richman et al., 1975; Chi et al., 1977; Armstrong et al., 1995). Gender-specific rates of brain maturation (Geschwind and Galaburda, 1985) may partly account for present findings of sexual dimorphism in local gyrification, although the details of this relationship require further examination. Genetic determination and/or the differential effects of gonadal hormones during brain growth are likely to affect the gender-specific emergence of local gyrification (Arnold and Gorski, 1984; Breedlove, 1994; Goldstein et al., 2001; Thompson et al., 2001). However, given that brain growth is partly confined by the size of the intracranial cavity (Hofman, 1989; Van Essen, 1997; Courchesne et al., 2000), increased gyrification in female brains might alternatively (or additionally) be caused by a greater constraint of brain expansion due to smaller skull sizes in women.

Acknowledgments

This work was supported by research grants R01 LM005639 (funded by the NLM and NIA) and P01 EB001955 (funded by the NIBIB, NINDS, and NIMG), an NIMH NRSA Training Grant (MH14584) and a Daniel X. Freedman NARSAD Young Investigator Award (to KLN) and R21 grants RR19771 and EB01561 (to PMT). Additional support was provided by U54 RR021813 (funded by the NCRR, NCBC and NIGMS), P41 RR013642 and M01 RR000865 (funded by the NCRR). We thank Karen Schrock for proof reading the manuscript.

References

Armstrong, E., Schleicher, A., Omran, H., Curtis, M., Zilles, K., 1995. The ontogeny of human gyrification. Cereb. Cortex 5, 56–63.

Arnold, A.P., Gorski, R.A., 1984. Gonadal steroid induction of structural sex differences in the central nervous system. Annu. Rev. Neurosci. 7, 413–442.

Benjamini, Y., Hochberg, Y., 1995. Controlling the false discovery rate: a practical and powerful approach to multiple testing. J. R. Stat. Soc., B 57, 289–300.

Blanton, R.E., Levitt, J.G., Thompson, P.M., Narr, K.L., Capetillo-Cunliffe, L., Nobel, A., Singerman, J.D., McCracken, J.T., Toga, A.W., 2001. Mapping cortical asymmetry and complexity patterns in normal children. Psychiatry Res. 107, 29–43.

Breedlove, S.M., 1994. Sexual differentiation of the human nervous system. Annu. Rev. Psychol. 45, 389–418.

Caviness Jr., V.S., 1975. Mechanical model of brain convolutional development. Science 189, 18–21.

Chi, J.G., Dooling, E.C., Gilles, F.H., 1977. Gyral development of the human brain. Ann. Neurol. 1, 86–93.

Chung, M.K., Robbins, S.M., Dalton, K.M., Davidson, R.J., Alexander, A.L., Evans, A.C., 2005. Cortical thickness analysis in autism with heat kernel smoothing. NeuroImage 25, 1256–1265.

Courchesne, E., Chisum, H.J., Townsend, J., Cowles, A., Covington, J., Egaas, B., Harwood, M., Hinds, S., Press, G.A., 2000. Normal brain development and aging: quantitative analysis at in vivo MR imaging in healthy volunteers. Radiology 216, 672–682.

do Carmo, M.P., 1976. Differential Geometry of Curves and Surfaces. Englewood Cliffs, Prentice Hall, NJ.

Geschwind, N., Galaburda, A.M., 1985. Cerebral lateralization. Biological mechanisms, associations, and pathology: II. A hypothesis and a program for research. Arch. Neurol. 42, 521–552.

Goldman-Rakic, P.S., 1981. Prenatal formation of cortical input and development of cytoarchitectonic compartments in the neostriatum of the rhesus monkey. J. Neurosci. 1, 721–735.

Goldstein, J.M., Seidman, L.J., Horton, N.J., Makris, N., Kennedy, D.N., Caviness Jr., V.S., Faraone, S.V., Tsuang, M.T., 2001. Normal sexual dimorphism of the adult human brain assessed by in vivo magnetic resonance imaging. Cereb. Cortex 11, 490–497.

Good, C.D., Johnsrude, I., Ashburner, J., Henson, R.N., Friston, K.J., Frackowiak, R.S., 2001. Cerebral asymmetry and the effects of sex and handedness on brain structure: a voxel-based morphometric analysis of 465 normal adult human brains. NeuroImage 14, 685–700.

Halpern, D.F., 1992. Sex Differences in Cognitive Abilities. Erlbaum, Hillsdale, NJ.

Hofman, M.A., 1989. On the evolution and geometry of the brain in mammals. Prog. Neurobiol. 32, 137–158.

Kimura, D., 1999. Sex and Cognition. MIT-Press, Boston.

Luders, E., Narr, K.L., Thompson, P.M., Rex, D.E., Jancke, L., Steinmetz, H., Toga, A.W., 2004. Gender differences in cortical complexity. Nat. Neurosci. 7, 799–800.

MacDonald, D., A Method for Identifying Geometrically Simple Surfaces from Three Dimensional Images. PhD thesis McGill University, Montreal.

MacDonald, D., Avis, D., Evans, A., 1994. Multiple surface identification and matching in magnetic resonance imaging. Proc.-SPIE 2359, 160–169.

Magnotta, V.A., Andreasen, N.C., Schultz, S.K., Harris, G., Cizadlo, T., Heckel, D., Nopoulos, P., Flaum, M., 1999. Quantitative in vivo measurement of gyrification in the human brain: changes associated with aging. Cereb. Cortex 9, 151–160.

Mazziotta, J.C., Toga, A.W., Evans, A., Fox, P., Lancaster, J., 1995. A probabilistic atlas of the human brain: theory and rationale for its development. The International Consortium for Brain Mapping (ICBM). NeuroImage 2, 89–101.

Narr, K.L., Bilder, R.M., Kim, S., Thompson, P.M., Szeszko, P., Robinson, D., Luders, E., Toga, A.W., 2004. Abnormal gyral complexity in first-episode schizophrenia. Biol. Psychiatry 55, 859–867.

Narr, K.L., Bilder, R.M., Toga, A.W., Woods, R.P., Rex, D.E., Szeszko, P.R., Robinson, D., Sevy, S., Gunduz-Bruce, H., Wang, Y.P., DeLuca, H., Thompson, P.M., 2005. Mapping cortical thickness and gray matter concentration in first episode schizophrenia. Cereb. Cortex 15, 708–719.

Nopoulos, P., Flaum, M., O'Leary, D., Andreasen, N.C., 2000. Sexual dimorphism in the human brain: evaluation of tissue volume, tissue composition and surface anatomy using magnetic resonance imaging. Psychiatry Res. 98, 1–13.

Rademacher, J., Caviness Jr., V.S., Steinmetz, H., Galaburda, A.M., 1993. Topographical variation of the human primary cortices: implications for neuroimaging, brain mapping, and neurobiology. Cereb. Cortex 3, 313–329.

Rakic, P., 1988. Specification of cerebral cortical areas. Science 241, 170–176.

Richman, D.P., Stewart, R.M., Hutchinson, J.W., Caviness, V.S., 1975. Mechanical model of brain convolutional development. Science 189, 18–21.

Rilling, J.K., Insel, T.R., 1999. The primate neocortex in comparative perspective using magnetic resonance imaging. J. Hum. Evol. 37, 191–223.

Roland, P.E., Zilles, K., 1994. Brain atlases—A new research tool. Trends Neurosci. 17, 458–467.

Shattuck, D.W., Leahy, R.M., 2002. BrainSuite: an automated cortical surface identification tool. Med. Image Anal. 6, 129–142.

Sled, J.G., Zijdenbos, A.P., Evans, A.C., 1998. A nonparametric method for automatic correction of intensity nonuniformity in MRI data. IEEE Trans. Med. Imag. 17, 87–97.

Sowell, E.R., Thompson, P.M., Leonard, C.M., Welcome, S.E., Kan, E., Toga, A.W., 2004. Longitudinal mapping of cortical thickness and brain growth in normal children. J. Neurosci. 24, 8223–8231.

Thompson, P.M., Schwartz, C., Lin, R.T., Khan, A.A., Toga, A.W., 1996a. Three-dimensional statistical analysis of sulcal variability in the human brain. J. Neurosci. 16, 4261–4274.

Thompson, P.M., Schwartz, C., Toga, A.W., 1996b. High-resolution random mesh algorithms for creating a probabilistic 3D surface atlas of the human brain. NeuroImage 3, 19–34.

Thompson, P.M., Cannon, T.D., Narr, K.L., van Erp, T., Poutanen, V.P., Huttunen, M., Lonnqvist, J., Standertskjold-Nordenstam, C.G., Kaprio, J., Khaledy, M., Dail, R., Zoumalan, C.I., Toga, A.W., 2001. Genetic influences on brain structure. Nat. Neurosci. 4, 1253–1258.

Thompson, P.M., Lee, A.D., Dutton, R.A., Geaga, J.A., Hayashi, K.M., Eckert, M.A., Bellugi, U., Galaburda, A.M., Korenberg, J.R., Mills, D.L., Toga, A.W., Reiss, A.L., 2005. Abnormal cortical complexity and thickness profiles mapped in Williams syndrome. J. Neurosci. 25, 4146–4158.

Van Essen, D.C., 1997. A tension-based theory of morphogenesis and compact wiring in the central nervous system. Nature 385, 313–318.

Watson, J.D., Myers, R., Frackowiak, R.S., Hajnal, J.V., Woods, R.P., Mazziotta, J.C., Shipp, S., Zeki, S., 1993. Area V5 of the human brain: evidence from a combined study using positron emission tomography and magnetic resonance imaging. Cereb. Cortex 3, 79–94.

Woods, R.P., Grafton, S.T., Watson, J.D., Sicotte, N.L., Mazziotta, J.C., 1998. Automated image registration: II. Intersubject validation of linear and nonlinear models. J. Comput. Assist. Tomogr. 22, 153–165.

Yucel, M., Stuart, G.W., Maruff, P., Velakoulis, D., Crowe, S.F., Savage, G., Pantelis, C., 2001. Hemispheric and gender-related differences in the gross morphology of the anterior cingulate/paracingulate cortex in normal volunteers: an MRI morphometric study. Cereb. Cortex 11, 17–25.

Zilles, K., Armstrong, E., Schleicher, A., Kretschmann, H.J., 1988. The human pattern of gyrification in the cerebral cortex. Anat. Embryol. (Berl) 179, 173–179.